



Article submitted to journal

Subject Areas:

xxxxx, xxxx, xxxx

Keywords:

Sensory feedback system, tactile sensors, electronic skin, electrotactile stimulation, Teleportation

Author for correspondence:

Yahya Abbass

e-mail: yahya.abbass@edu.unige.it

Full-hand electrotactile feedback using electronic skin and matrix electrodes for high-bandwidth human-machine interfacing

Yahya Abbass¹, Strahinja Dosen², Lucia Seminara¹, and Maurizio Valle¹

¹Department of Electrical, Electronic, Telecommunications Engineering, and Naval Architecture (DITEN), University of Genoa, 16145, Genova, Italy.

²Department of Health Science and Technology, Aalborg University, Aalborg, Denmark

Tactile feedback is relevant in a broad range of human-machine interaction systems (e.g., teleoperation, virtual reality and prosthetics). The available tactile feedback interfaces comprise few sensing and stimulation units, which limits the amount of information conveyed to the user. The present study describes a novel technology that relies on distributed sensing and stimulation to convey comprehensive tactile feedback to the user of a robotic end-effector. The system comprises six flexible sensing arrays (57 sensors) integrated on the fingers and palm of a robotic hand, embedded electronics (64 recording channels), a multichannel stimulator, and seven flexible electrodes (64 stimulation pads) placed on the volar side of the subject's hand. The system was tested in seven able-bodied subjects asked to recognize contact positions and identify contact sliding on the electronic skin, using distributed (DAC) and single dedicated (SAC) anode configurations. The experiments demonstrated that DAC resulted in substantially better performance. Using DAC, the system successfully translated the contact patterns into electrotactile profiles that the subjects could recognize with satisfactory accuracy (88.57{11} % for static and 93.3{5} % for dynamic patterns). The proposed system is an important step towards the development of a high-density human-machine interfacing between the user and a robotic hand.

1. Introduction

Human-machine interface that connects a human operator and an artificial system (e.g., robot, or virtual avatar) is the key element for achieving seamless interaction. Ideally, such an interface should transmit commands from the human to the artificial system as well as sensor information from that system back to the operator to provide feedback and close the control loop. For instance, haptic feedback can enrich interaction fidelity and facilitate the feeling of immersion when interacting with a virtual world or controlling a remote robotic system [1,2].

In teleoperation, haptic interfaces in the form of desktop devices, hand exoskeletons, data gloves and tactile displays have been proposed [3]. Interaction forces detected by the robot can be transmitted to the operator (kinaesthetic feedback) using exoskeletons that can be mounted on the hand [4–9], or over the full arm [10], and some solutions are already commercially available (e.g., CyberGrasp from CyberGlove Systems, CA). Although such kinaesthetic systems provide most realistic feedback, they are also cumbersome, complex and expensive. An alternative approach, which can substantially simplify the design of the interface is to transmit feedback information using tactile stimulation delivered through miniature vibration motors [11,12] or tactors [12–14]. These techniques have been extensively described and compared in several recent reviews [13]. For example, in [15], a vibrotactile display system stimulating the fingertip through a 4×4 array of tactors was developed and integrated on an Omega7 force feedback device for the teleoperation of an LWR KUKA manipulator. Authors in [16] equipped a soft robotic hand with 6-axis force sensor and used two wearable vibrotactile armbands to convey information about collisions. Electrotactile stimulation, which relies on delivering low-intensity current pulses to activate skin afferents and elicit tactile sensations, was also used to provide feedback in teleoperation [17–26]. For instance, in [27] a feel-through interface “Tacttoo” consisting of an array of 8 equispaced circular electrodes was developed to stimulate the finger. Similarly, in [26] an electrode made by printing the conductive ink onto a flexible substrate has been developed to deliver both electrical stimulus and electrostatic force to the fingertip. A data glove enhanced with six stimulation electrodes placed on the dorsal side of the hand was used to deliver contact information from a mobile robot [24] and force from the end effector of a robotic arm [17]. Apart from teleoperation, tactile stimulation has been used to provide feedback to the user of a prosthetic hand [28–33], to improve utility [34] and promote feeling of embodiment [35], as well as, in virtual reality to establish an immersed experience by enabling users to sense virtual objects. Recently, in [36] the authors examined the impact of electrotactile stimulators and several types of vibrotactile actuators on mimicking touch interactions in virtual and augmented reality. Despite important developments, the conventional tactile feedback interfaces are characterized with a limited communication bandwidth. They rely on a few stimulation points, which limits the amount of information that can be transmitted to the user. Indeed, this is very different from the natural feedback provided by, e.g., human hand, which is covered with a dense network of tactile mechanoreceptors measuring spatially distributed contact information with high resolution.

To provide high resolution tactile information mimicking the human sense of touch, this information first needs to be measured by artificial systems integrating high-density network of sensing units. For example, authors in [37] developed a scalable tactile glove with 548 sensors distributed all over the hand. The glove was used to identify individual objects, estimate their weight, and explore the typical tactile patterns that emerge while grasping objects. Many other electronic skins (e-skin) have been developed [38–45] and successfully applied in robotics [46–49], prosthetics [50–57], and health-monitoring technologies [58,59]. However, to the best of our knowledge, none of the developed e-skins has been integrated into a feedback system to deliver touch information to robotic hand operators or prosthetic users. Instead, the previous studies were mostly focused on the fabrication of the e-skin and its deployment in tactile data extraction and classification. The use of such a high-density e-skin in the online feedback loop to the human subject, however, requires tackling different challenges such as the development of powerful electronics and tactile data processing methods while minimizing latency in the

feedback system. However, a critical question still remains: how to convey the rich tactile information recorded by a high-density e-skin as the feedback to the user. This challenge can be tackled by using electrotactile stimulation, as this technology leads to compact design and allows printing electrodes in different shapes, sizes and configurations of the conductive pads (stimulation points) for the stimulation of different parts of the user body [60]. For instance, in tactile feedback for a prosthesis, the electrode is shaped to cover the residual limb [60], while for the applications in teleoperation and virtual reality the electrode needs to be placed on the user's hand [61].

Endowing an end effector with a distributed sensing system combined with distributed feedback system would enable high-bandwidth bilateral communication between the user and the machine/computer. Our recent research efforts are directed towards developing such a high-bandwidth feedback system [62,63]. The system described in [63] comprised a single sensing array (with 16 sensors) integrated on the index finger of the mockup¹ of the Michelangelo prosthetic hand, a 32 channel embedded electronics for signal acquisition and conditioning, a multichannel electrotactile stimulator, and a matrix electrode (with 24 pads) placed on the subject's forearm. The system developed in [63] was used to provide electrotactile feedback from the single sensorized finger to the subject's forearm, which is of interest for the provision of tactile feedback to a user of a hand prosthesis. Preserving the same sensing principle based on PVDF piezoelectric polymers, the present manuscript describes further development of this initial solution into a feedback interface that conveys comprehensive full-hand tactile information (all fingers and palm). In particular, the system captures contact events (binary values) using the e-skin integrated on the fingers and palm of a robotic hand (mockup) and delivers this tactile information to the subject using stimulation pads distributed over the fingers and palm of his/her hand. This setup is of interest, for instance, in telemanipulation scenarios, to provide a comprehensive feedback to an operator of a remote robotic gripper. To achieve this, we have integrated six sensing arrays (57 sensors) on the fingers and palm of the mockup of the Michelangelo hand, and developed an extended version of the embedded electronics to acquire, process and transmit tactile data from the novel sensor matrix. Furthermore, the present manuscript describes a novel electrode, designed and printed specifically to allow the delivery of high-density electrotactile feedback to the fingers and palm of the human hand (operator), with the stimulation pads mimicking the arrangement of the sensing units on the robotic hand. To the best of our knowledge, this is the first system that conveys high-resolution tactile information from the whole dorsum of a robotic hand to the whole dorsum of a human hand. The present work presents the challenges that need to be tackled for the successful implementation of such a system, including the design of sensing and stimulation arrays, tactile signal processing, mapping between sensing and stimulation pads, and approaches for electrode configuration.

Importantly, since providing such a comprehensive high-resolution feedback to the human hand is in itself a novelty, the optimal electrode configuration is not yet established. The common anode, for instance, can be distributed within the electrode or placed outside of the hand as a dedicated pad. Both configurations were used previously [27,64–66] but the assessment in these studies was limited to the fingertip, rather than the whole hand, and the two configurations were not systematically compared. The present study, therefore, reports on the validation of the sensing system as well as on the psychometric assessment of the whole-hand feedback. The psychometric tests were conducted to compare the two anode configuration methods as well as to assess the ability of the proposed system to capture and deliver distributed tactile information as the online feedback to the subject.

The paper is organized as follows: Section 2 illustrates materials and methods. Section 3 presents the validation of the sensing system. Section 4 describes the experimental protocol for psychometric assessment of the developed feedback system. The results of the psychometric assessment are reported in Section 5. Finally, our discussion and conclusive remarks are given in Section 6.

¹The mockup is a rigid 3D printed copy of the Michelangelo hand in real size.

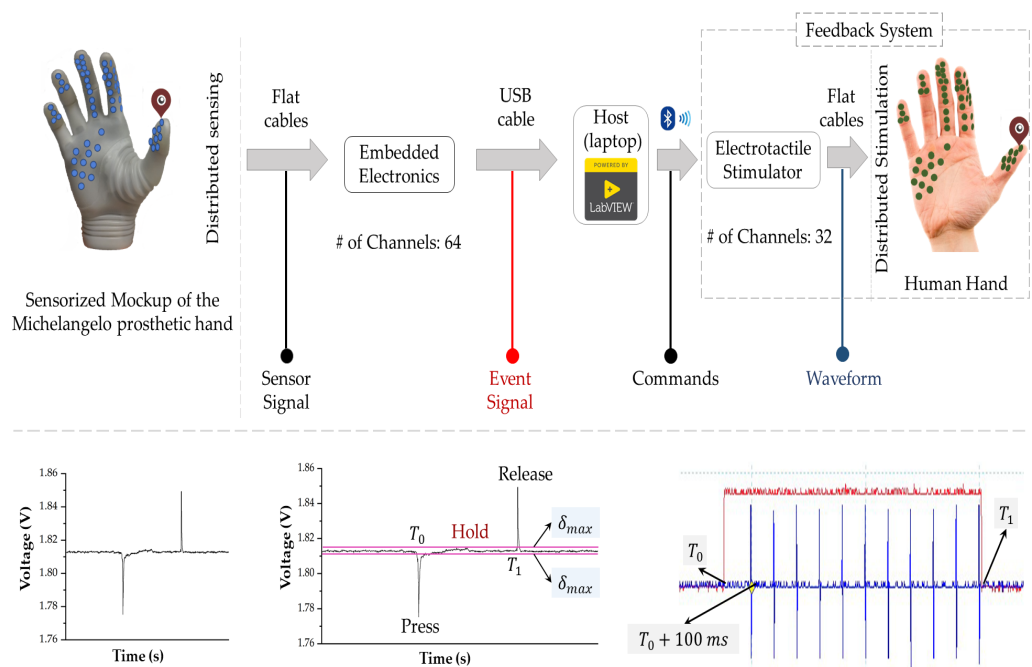


Figure 1. Top: System structure. The system comprises an e-skin including 57 sensors, embedded electronics for signal acquisition, processing and communication, and a multichannel electrotactile stimulator with flexible matrix electrodes (32 electrode pads). Bottom: The online operation of the feedback system. The black signal (left) corresponds to a sensor output due to a specific type of contact ("long press"). The embedded electronics uses two thresholds to detect press and release, and based on that generate the event signal (red signal) and send it to the host PC. The PC sends commands to the stimulator and the train of stimulation pulses (blue signal) is delivered through the corresponding electrode pad as tactile feedback to the subject's hand.

2. Materials and Methods

(a) System Description

The proposed system (figure 1) includes: 1) piezoelectric sensing arrays (electronic skin), 2) embedded electronics for signal acquisition and conditioning, 3) electrotactile stimulator, 4) flexible surface electrodes, and 5) host laptop PC (1.9 GHz, 16 GB). The e-skin converts mechanical contact into a set of electrical signals (one signal per sensor). Sensor signals are sampled by the embedded electronics, processed, and sent to the host PC. The signals are then filtered and when sensor output exceeds a given threshold contact events are detected, and the activated sensors are highlighted on the graphical user interface on the PC (visual feedback). This information is used to set the state (on/off) of the corresponding stimulation channels (mapping between sensors and stimulation pads is presented in section 2(b)). The PC generates appropriate stimulation commands and sends them to the stimulator via Bluetooth. The electrotactile stimulation is delivered to the subject through matrix electrodes placed on the volar side of the hand. As the feedback pipeline runs in real-time, the tactile interaction recorded by the electronic skin is translated online into dynamic tactile sensations elicited across the subject's hand. Figure 1 (Bottom) illustrates the online pipeline of the system, which was implemented following the approach presented in [63].

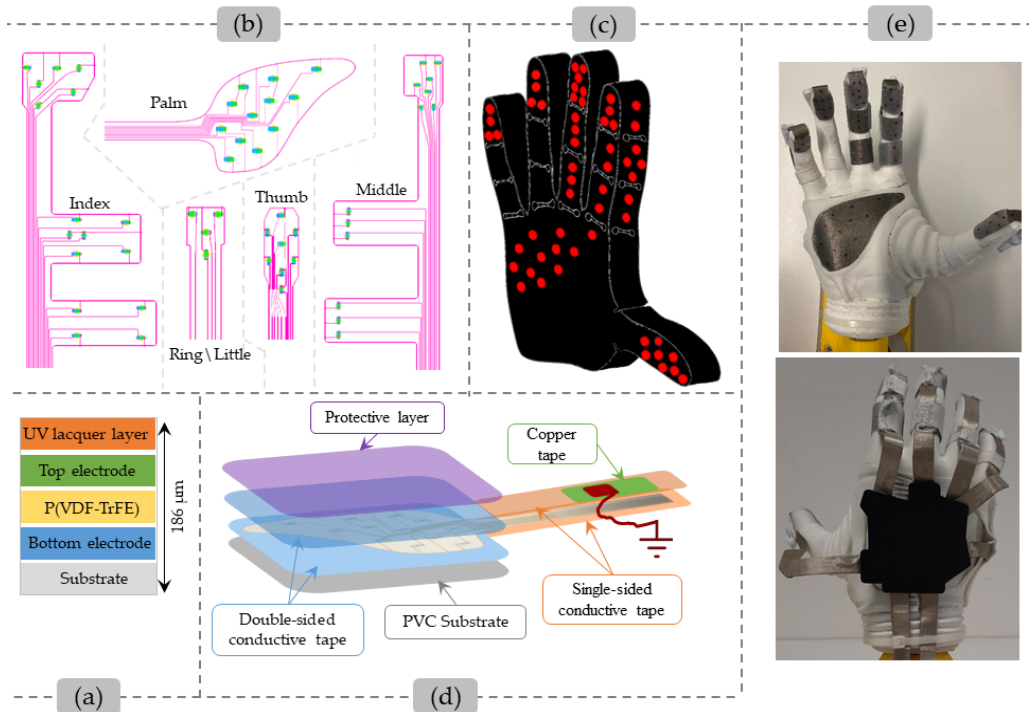


Figure 2. (a) Single sensor structure. (b) Layout of the sensing arrays for the fingers and palm of the Michelangelo robotic hand. (c) Sensor distribution over the hand. (d) Skin patch. (e) Sensing system integrated on the mockup of the Michelangelo hand (front and back views).

(i) Sensorized mockup of the Michelangelo hand

- **Tactile sensor arrays:**

Figure 2a shows the structure of a single sensor. A ferroelectric polymer P(VDF-TrFE) layer (5.1 μm thick) was sandwiched between PEDOT: PSS conductive layers and then covered with a UV-curable lacquer layer for overall sensor protection. The whole structure was screen printed on a transparent and flexible PET (175 μm thick) substrate. The fabrication technology was presented and validated in [67]. It is worth noting that piezoelectric polymer sensors have a bandwidth integrating those of all mechanoreceptors in the human skin. This kind of sensors have potentialities to measure dynamic contacts over the whole range of the tactile application and to infer information about static contact by data processing. A complete set of sensing arrays with different geometries and sensor distributions was developed to fit the fingers and palm of a Michelangelo prosthetic hand [68]. Figure 2b shows the geometry, sensor distribution, and size of the sensing arrays while figure 2c highlights sensor distribution over the fingers and palm of a mockup of the Michelangelo hand. The finger sensing arrays were designed to easily fit on the phalanges. Due to its prominent role in grasping and manipulation [69], the index finger was covered most extensively with the sensors. Specifically, sensors were distributed on the volar and lateral sides of the fingertip (4 and 2 sensors, respectively), and the middle (2 and 4 sensors), and proximal (2 and 2 sensors) phalanges. The sensors on the lateral aspect were added to allow for contact detection when lateral grasp is used, in which an object is grasped between the volar aspect of the thumb and the lateral side of the index. Similarly, the middle finger was provided with 13 sensors covering the fingertip (7 sensors), and the middle (3 sensors), and proximal (3 sensors) phalanges. The fingertips of the thumb, ring, and little

fingers were equipped with 8, 4, and 4 sensors, respectively. Finally, 12 sensors were distributed over the palm.

- **Sensor Integration:**

In this particular work, a mockup of the Michelangelo robotic prosthetic hand is used as an example of a robotic hand. This passive version of the Michelangelo hand was 3D printed using P.L.A (polylactic acid) thermoplastic polyester with the Fused Deposition Modeling (FDM) technique. Sensing arrays reported in figure 2b require an additional fabrication step to realize skin patches that can be integrated onto the hand. Figure 2d shows the structure of the skin patch for the palm. The sensing arrays were integrated on the mockup following the same approach described in [63]. The arrays were shielded using conductive tapes (Model tesa 60262) and then protected using a thin flexible protective layer (Art. 5500 Dream, Framisitalia). The structure was mounted on a flexible substrate (i.e. PVC in Fig. 2d) and then wrapped around the fingers and the palm of the mockup. The shielding layers were connected to the ground reference of the embedded electronics (see section 2(a)(ii)) using a self-adhesive copper foil tape and a wire. All six sensing arrays were integrated on the mockup following the aforementioned procedure.

Figure 2e shows the complete sensing system integrated on the mockup. Four shielded FPC cables were used to connect the PCB to the embedded electronics. All the materials used in the integration process (i.e., substrates and protective layers) have been designed and developed by SMARTEX [70].

(ii) Embedded Electronics

The embedded electronics used in this study is an extended version of the systems presented in [63, 71]. Compared to the previous design that can accommodate up to 32 sensors, the current design can handle up to 64 sensors through two daisy-chained analog-to-digital converters (DDC232, Texas Instruments) [72] mounted on the top and bottom side of the PCB. The two DDC232 were daisy chained in order to avoid data loss during the acquisition process. Four sockets (2 on the top side and 2 on the bottom side) acquire signals from 64 sensors where each block accommodates 16 sensors. BL600 module is used to read, process, and transmit sensor data. Our solution provides more channels with respect to analogous state-of-the-art electronic systems to acquire and process data from piezoelectric tactile sensors for touch sensing with robotic hands. In particular, the interface electronics for the system on chip device for prosthetic applications presented in [73] offers thirteen channels only, while the voltage-mode approach to read PVDF taxel outputs proposed in [49] only manages data from nine sensors.

In the present study, the embedded electronics was configured to collect and process tactile data from 57 sensors at 2K samples/s. The 2 kHz sampling rate was used to capture the full bandwidth of the sensor (see section 2(a)(i)), which is beneficial for detecting the onset of contact events characterized by a steep increase/decrease in the signal. An Exponential Moving Average (EMA) digital filter was implemented in the firmware of the embedded electronics to filter signals from the sensors. To enable the system to detect contact events, the Detection Thresholds (DT) of the 57 sensors were first determined. To this aim, the interface electronics recorded signals from the skin for approx. 3-s with no contact. The DTs were set to the lowest (δ_{min}) and the highest amplitude (δ_{max}) of the filtered signals measured during the 3-s calibration period. Exceeding those thresholds was used as an indication that contact and release occurred, respectively. As an example, figure 1 (bottom) shows the filtered voltage signal of a single sensor generated in response to a press-hold-release contact as well as the corresponding event signal that controls the start and stop of the stimulation delivered to the subject's hand.

(iii) Feedback System

- **Electrotactile Stimulator**

The feedback interface employs a 32-channel programmable battery-powered stimulator ('Tactility', Tecnalia Research and Innovation, Spain [74]). The stimulator generates biphasic

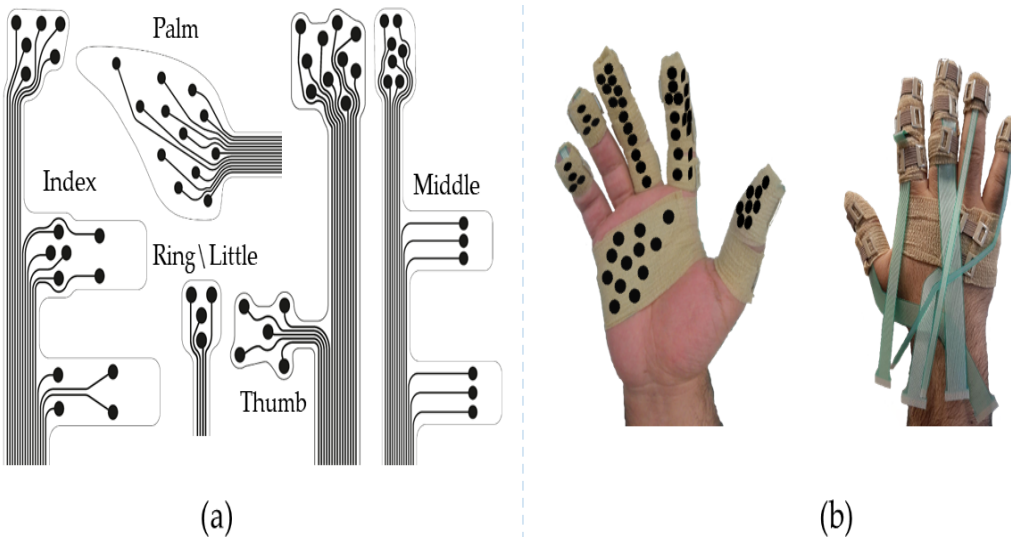


Figure 3. Flexible electrodes for the electrotactile stimulation of the hand. (a) Layout of the pad arrays to cover the fingers and palm. (b) Volar and dorsal view of a human hand covered with the electrode arrays. Stimulation pads are indicated as black dots (volar) and rectangles (later index).

symmetric current- pulses that are distributed in time and space over 32 channels. The stimulator is fully programmable, and the stimulation parameters can be adjusted online by sending text commands from the host PC via a Bluetooth connection. The amplitude of the current pulses can be modulated in the range of 0–10 mA with increments of 0.1 mA, the pulse width, from 50 to 5000 μ s in steps of 10 μ s; the frequency resolution is 1 Hz with the maximum rate of 400 Hz. Each stimulation channel could be set to act as anode or cathode.

In the present study, the PC sends stimulation commands to the stimulator to activate/deactivate the stimulation through the respective electrode pads. Specifically, the stimulation is activated by a press and deactivated by a release event (see figure 1). The output channels of the stimulator were connected to a small PCB that routes 32 stimulation channels to 64 pads of the electrode, as described in the next section.

• Electrodes

As explained in Introduction, providing a comprehensive tactile feedback using a large number of pads distributed over the whole hand (palm and fingers) is a novel application, which has not been explored before. Matrix electrodes have been used to provide electrotactile feedback to the hand [20,65,75,76]. However, the stimulation was mostly localized to the fingertip. The aim of this study was to provide spatially distributed high-resolution feedback to the hand, which is spatially congruent to the mechanical interaction detected by the e-skin. Therefore, a custom-made electrode that covers the whole hand needed to be designed. Therefore, in the present study, the stimulator was connected to six flexible matrix electrodes developed by Tecnalia Research and Innovation. The electrodes are made of a polyester layer, an Ag/AgCl conductive layer, and an insulation coating covering the conductive leads. Pad distributions on the six electrodes are shown in figure 3a. The electrodes were designed to be placed on the human hand and the pad distribution mirrors the design of the sensing arrays (see section 2(a)(i)). Sixty four circular pads were distributed over 6 electrodes in total (5 electrodes for the fingers and one electrode for the palm, figure 3b).

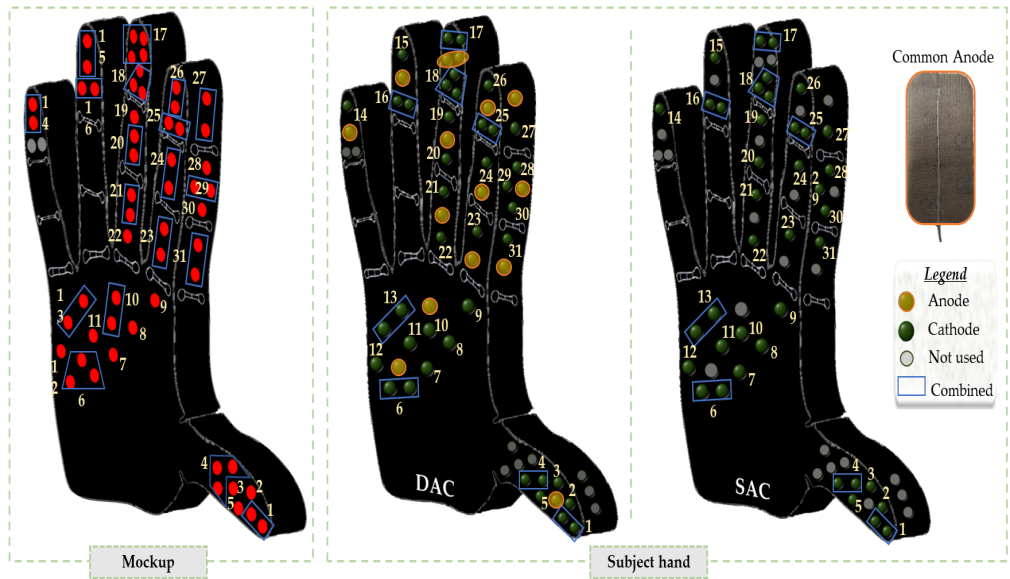


Figure 4. The arrangement of the sensors on the e-skin (left) and the distributions of the cathode and anode pads on the electrode arrays placed on the subject's hand (center and right). The numbers on the e-skin and electrode array indicate the mapping of sensor sets to corresponding groups of pads connected to a single stimulation channel. Two anode configurations were considered: a distributed anode comprised of a subset of pads (DAC, center), and a single dedicated electrode placed on the dorsal side of the hand (SAC, right).

(b) Mapping Sensors to Pads

The electrotactile stimulator used in the current study has 32 stimulation channels while the electrode arrays integrate 64 pads. Therefore, some electrode pads were grouped together and driven by a same stimulation channel. In addition, a reference electrode (anode) needed to be defined to close the stimulation circuit. To this aim, a small PCB was developed to route the pads to the channels and to implement two anode configurations (figure 4). The first configuration features an anode that was embedded within the electrode: in this case, 15 pads distributed over the volar side of the phalanges and the palm (distributed anode configuration, DAC) were connected to one of the stimulation channels configured as the anode, while the rest of the pads were connected to the remaining 31 channels configured as cathodes. This configuration was selected in order to localize the current flow, from a cathode to its closest anode segment, eliciting thereby a localized tactile sensation. A second configuration consists of a single large anode placed on the dorsal side of the hand (single anode configuration, SAC). It is important to note that the number of cathodes was identical in both configurations, as the distributed anodes were deactivated (unused) in the SAC configuration. In the present study, we compared the effectiveness of the two configurations (see section 4(a)(i)).

To map 57 tactile sensor outputs to the 31 channels of the stimulator, some neighboring sensors were grouped together and connected to a same stimulation channel. The mapping between sensor sets and groups of electrode pads is shown in figure 4 (left). The stimulation channel connected to a group of pads was activated if any of the sensors belonging to the corresponding sensor set detected a contact event.

Table 1. System features

Component	Feature	Specifications
Sensorized mockup	Number of Sensors	57 (distributed on the fingers and palm of the mockup)
	Sensor frequency bandwidth	1-1kHz
	Size	4.8 cm × 3 cm
	Number of channels	64
Embedded Electronics	Sampling Rate	Up to 6K samples/second
	Connectivity	USB-C port communication interface and Bluetooth
	Power consumption	200 mW
	Overall Latency	100 ms
Feedback System	Connectivity	USB and Bluetooth
	Number of stimulation pads	64 (distributed on the fingers and palm of the hand of the participant)

3. Sensing System Demonstration

To assess that the sensors properly responded, validation experiments were conducted. In the first test, the experimenter holding a pen performed indentation tests by applying press-hold-release patterns on all 57 sensors, one at a time. In the second test, the experimenter used two pens to apply the press-hold-release pattern on two sensors simultaneously. Finally, the experimenter performed shear tests by applying a sliding pattern along the e-skin following specific sliding directions. In order to visualize the response of the sensing system, the embedded electronics was configured to acquire, filter, and send signals generated by the sensors to a host PC through USB. A LabVIEW software was developed to receive, visualize and save the tactile signals.

Table 1 summarizes the specifications of the different components of the system. In particular, the embedded electronics consumes 200 mW while continuously sampling and processing tactile signals and sending commands to the host. When supplied with a single 2 Ah Lithium polymer battery with a voltage of 3.7 V, the battery lifetime expectancy is 24 h.

Representative results from the sensing system validation experiments are shown in figure 5. The figure depicts the electrical response of six sensors to indentation tests (figures 5a-c) and to shear tests (figure 5d), as defined above. Figure 5a and figure 5b show the six sensors capturing the dynamic features of the mechanical event by generating two phasic bursts in charge-mode output signals. The bursts correspond to the press and release events, while there was almost no response in-between. The contact onset is associated to a decrease whereas contact release generates a signal increase. The signal peaks are arranged in sequence reflecting the fact that the touches were applied to the sensors sequentially. Figure 5c shows that the sensing system can capture multiple touches when they were applied simultaneously. Finally, figure 5d shows a sliding pattern that started on the palm, crossed the volar side of the index finger and ended on the fingertip of the index finger. The plot indicates that the six sensors respond to shear tests and that the sliding

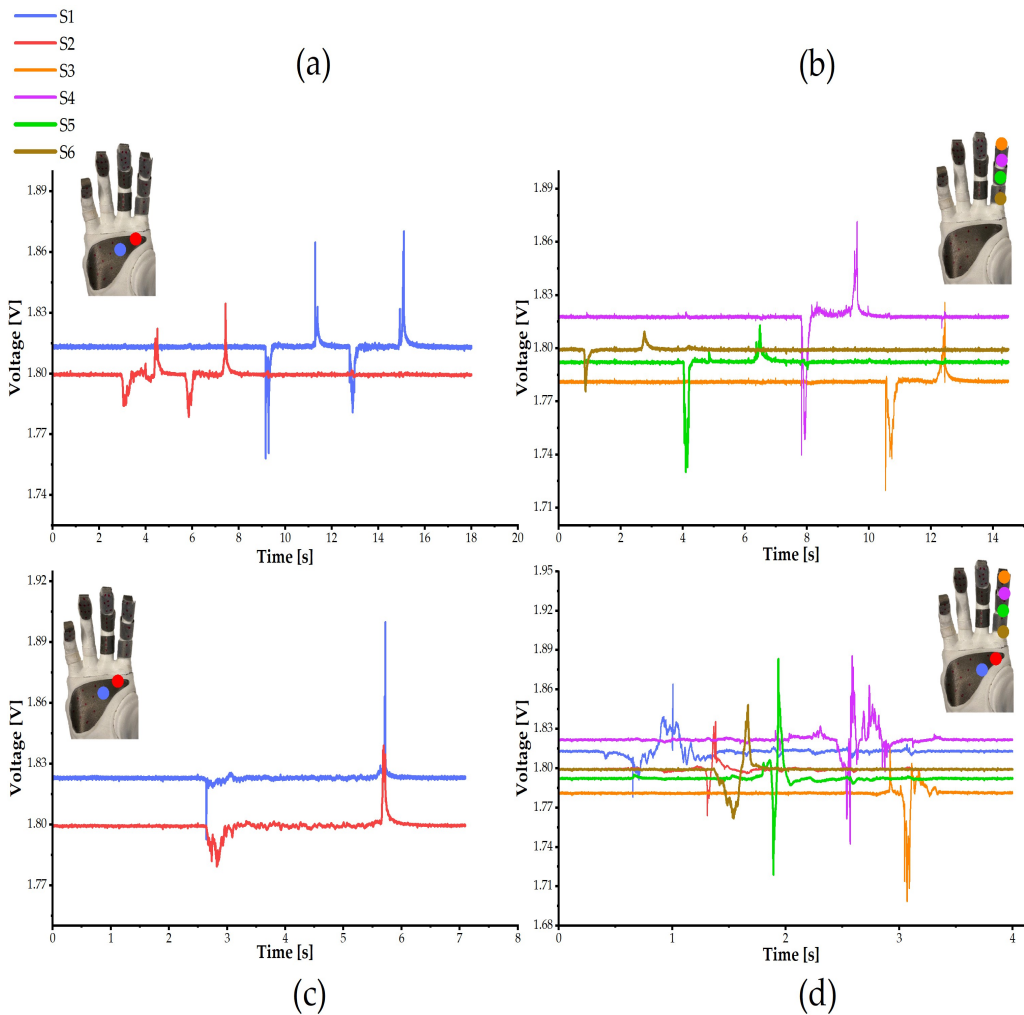


Figure 5. Illustrative data showing sensor outputs. Signals from six sensors are shown during touch interactions. The legend attributes colours to each specific sensor output. Indentation tests: (a) long press on two sensors located on the palm; (b) long press on the three phalanges of the index finger starting from the proximal phalange; (c) long press on two sensors (on the palm) at the same time. Shear tests: (d) sliding movement starting from the palm and moving toward the tip of the index finger.

direction could be easily inferred from the sequence of sensor activations. Interestingly, the sensor response pattern is in this case more complex; the press and release peaks are still visible, but they are not as sharp as in figure 5a and figure 5b. This reflects a different sensor response to the different type of mechanical interaction (shear forces). The sliding movement provoked more gradual activation and deactivation of the sensors compared to previous indentation tests. A number of interesting patterns are shown in figure 5d. They can actually reveal how shear information on the surface of the skin is translated into normal stress that is measured by the piezoelectric polymer sensors working in thickness mode. While in such a configuration PVDF polymer sensors only measure the normal T_{33} stress component [77], we have previously proven [78] that shear information on the skin surface can be also detected by the sensors. As a matter of fact, shear forces tend to unbalance the normal stress distribution on the substrate (where sensors are integrated) by producing a kind of wake in the direction of their resultant. Ahead of the wake the compression is increased while at the rear a tensile region appears. However, this previous

Table 2. Summary of experiments

Name	Anode configuration	Description	Touch patterns
<i>Static patterns</i>	SAC	Spatial coding with 21 classes (static patterns)	<u>Single touch:</u> G1, G2, ..., G14 <u>Two simultaneous touches:</u> G4-G1, G4-G3, G5-G4, G5-G6, G5-G1, G3-G1, G5-G10
	DAC		
<i>Dynamic patterns</i>	DAC	Spatial coding with twelve classes (dynamic patterns)	<u>Single sliding line:</u> IV, IL, M, PF, PTh, FT, PM, PIV <u>Two simultaneous sliding lines:</u> IV-M, PIV-PM, PIV-PTh, PM-PTh

study has been made for static contacts, not dynamic ones. The current protective layer will also ultimately affect stress transmission to the piezoelectric polymer sensors. Pursuing the goal of thoroughly coding these patterns is not a minor undertaking and requires a new experimental study with a well-controlled setup. This will be the topic of a forthcoming publication.

4. Psychometric Assessment

(a) Experiments

Two experiments (table 2) were conducted to assess if the system could convey information on contact location (indentation tests) and on the sliding movement along and/or across fingers (shear tests). In both experiments, the stimulation was delivered to the subject according to the mapping described in section (2)(b) and shown in figure 4.

(i) Static pattern experiment (Exp-SP)

This experiment evaluated if the feedback system could successfully convey the information about static contacts to the subject. The sensor sets shown in figure 4 were divided into 14 groups and labelled as shown in figure 6 (left). The groups were defined to assess if the subject could recognize touch delivered to each of the important functional areas (fingertips and phalanges). Moreover, the test comprised single and double touch (see table 2), where the experimenter pressed the skin to activate a single group or two groups, respectively. In the latter case, the tested combinations of two groups were defined so that they are functionally relevant, i.e., they were expected to be activated when closing the hand using different grasp types (e.g., pinch, lateral grasp). The experiment was conducted twice, once with distributed anode and once with single dedicated anode.

(ii) Dynamic pattern experiment (Exp-DP)

The experiment evaluated if the system could successfully deliver information about moving contacts to the subject. The experimenter interacted with the e-skin to activate a sequence of pads. The movement patterns included sliding along the volar and lateral aspects of the index finger, and the volar aspect of all fingers and palm. Moreover, the test comprised applying single and

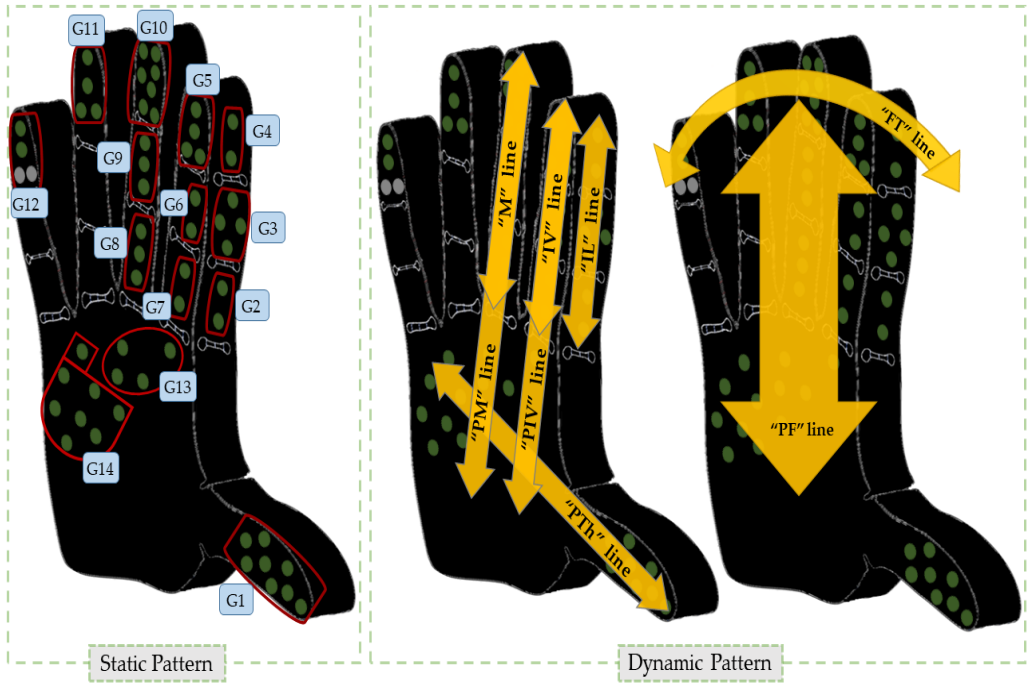


Figure 6. Left: Sensor distribution within the electronic skin placed on the fingers and palm of the mockup of the Michelangelo hand. The sensors were grouped into fourteen groups (G1-14, boxes). Right: Two psychometric experiments were conducted: 1- Exp-SP – skin indentation aligned on specific sensors (*Static pattern*) and 2- Exp-DP - shear tests (*Dynamic pattern*), i.e. sliding across Middle (M), Palm to Middle (PM), Index Volar side (IV), Index Lateral side (IL), Palm to Index Volar side (PIV), Palm to Thumb (PTh), Palm to Fingers (PF) and FingerTips (FT) lines in two directions.

double sliding lines (see table 2 and figure 6 (right)) shows the sliding patterns. Results from the Exp-SP experiment demonstrated that the DAC anode configuration performed significantly better than the SAC anode configuration. For that reason, in this experiment, the sliding lines were delivered to the subject using the DAC anode configuration only.

(b) Setup and Protocol

Seven healthy subjects (male, age 28 ± 4 years) participated in the two experiments described in section 4(a). Before starting, the subjects signed an informed consent form. Figure 7 shows the experimental setup. The subjects were seated comfortably on a chair in front of a monitor used for visualization. The forearm of the right arm was placed on a table surface and, the electrodes were placed on the fingers and palm of the subject's hand and secured with a self-adhesive bandage as shown in figure 3b. Each phalange was secured separately in order not to block the movements of the subject's fingers. Figure 7a shows the view from the subject perspective. The sensorized mockup of the Michelangelo hand was mounted on a support and placed so that the subject could not see the hand nor the experimenter interacting with the hand (see figure 7b). Before the experiments, the Sensation Thresholds (ST) were determined for each of the 31 pad groups (figure 4), using the methods of limits by varying the pulse amplitude value [79]. During the rest of the experiment, the pulse amplitude was set to $1.1 \times ST$, which ensured that the sensations elicited by the feedback were clear and comfortable. The amplitude was additionally fine-tuned by the experimenter until the subject reported that the perceived intensity was similar across the pad groups. The pulse rate and pulse width were common to all the pads and set to 50 Hz and 100 μ s, respectively. Each experiment started by introducing the subject to the sensory feedback system

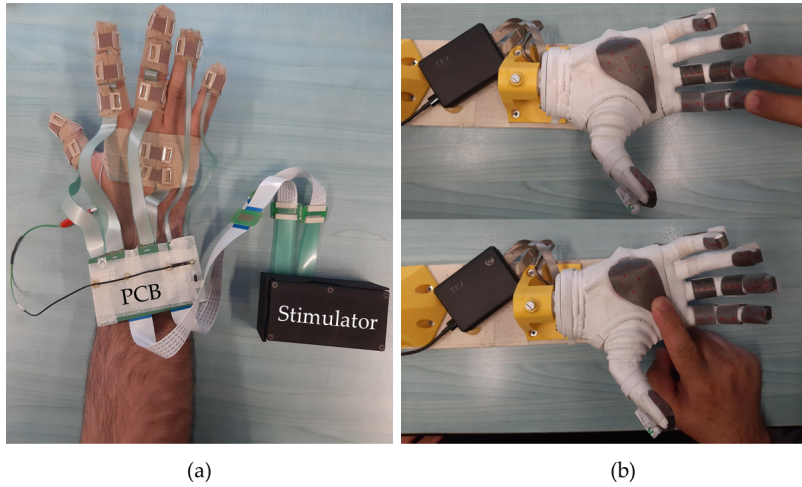


Figure 7. Experimental setup. (a) The subject received electrotactile feedback through electrode arrays placed on the right hand and covered with a medical bandage. The electrodes were connected to a small PCB routing 64 pads to 32 stimulation channels. The PCB includes a small jumper that was used to switch between the anode configurations, i.e., SAC and DAC. (b) Example of the experimenter interacting with the sensors: (bottom) the experimenter applies single touch on a set of sensors on the palm and (top) the experimenter touches the index and middle fingers simultaneously.

and feedback mapping. Both experiments (Exp-SP and Exp-DP) comprised three phases: learning, reinforced learning, and validation. In the learning phase, the patterns described in table 2 were delivered and the subjects were informed beforehand which pattern will be presented.

During reinforced learning, the contact patterns were randomly applied, while the subjects were asked to guess the applied patterns. The experimenter then provided verbal feedback on the correct answer by saying “correct” or “incorrect” and, in the latter case, disclosing the correct pattern. During the final validation phase, the patterns were again presented randomly, the subject verbally indicated the pattern, but no verbal feedback was given. Each stimulus was presented to the subject 3 times during the first two sessions and 5 times during the validation phase.

(c) Data Analysis

The outcome measure was the success rate (SR) defined as the percent of correctly recognized contact patterns, namely, activated groups in Exp-SP and sliding movements in Exp-DP. The SRs were computed per subject for each contact pattern. In Exp-SP, the SR obtained with DAC was compared to that achieved with SAC to test if the recognition was impacted by the anode configuration. The results of the tests are reported as median{interquartile range (IQR)}. The overall performance is also presented in the form of confusion matrices to identify prevalent mistakes.

The paired sample Wilcoxon signed rank test was applied to assess statistically significant differences between SAC and DAC. Non-parametric tests were used due to the small number of subjects. The threshold for the statistical significance was set at $p < 0.05$, and the statistical analysis was conducted in OriginPro 2018 (OriginLab, US).

5. Results

The box plot of the success rates (median{IQR}) from all the experiments are presented in figure 8. The subjects achieved a high overall success rate (both single and double touches) when recognizing the touched group of sensors (Exp-SP test) using DAC with median{interquartile

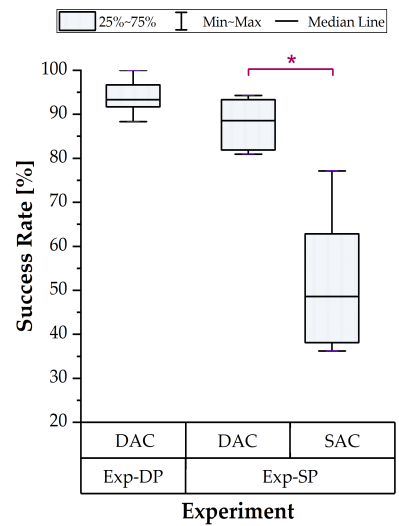


Figure 8. The overall success rate (SR) of recognizing sliding lines in experiment Exp-DP for DAC (left) and groups of sensors in Exp-SP experiment for SAC and DAC (right). Asterisks indicates the statistically significant difference in mean SR for the different anode configurations. (*, $p < 0.05$).

range} of 88.57{11} %). The SAC resulted in a significant drop ($p < 0.05$) in performance (48.57{25} %).

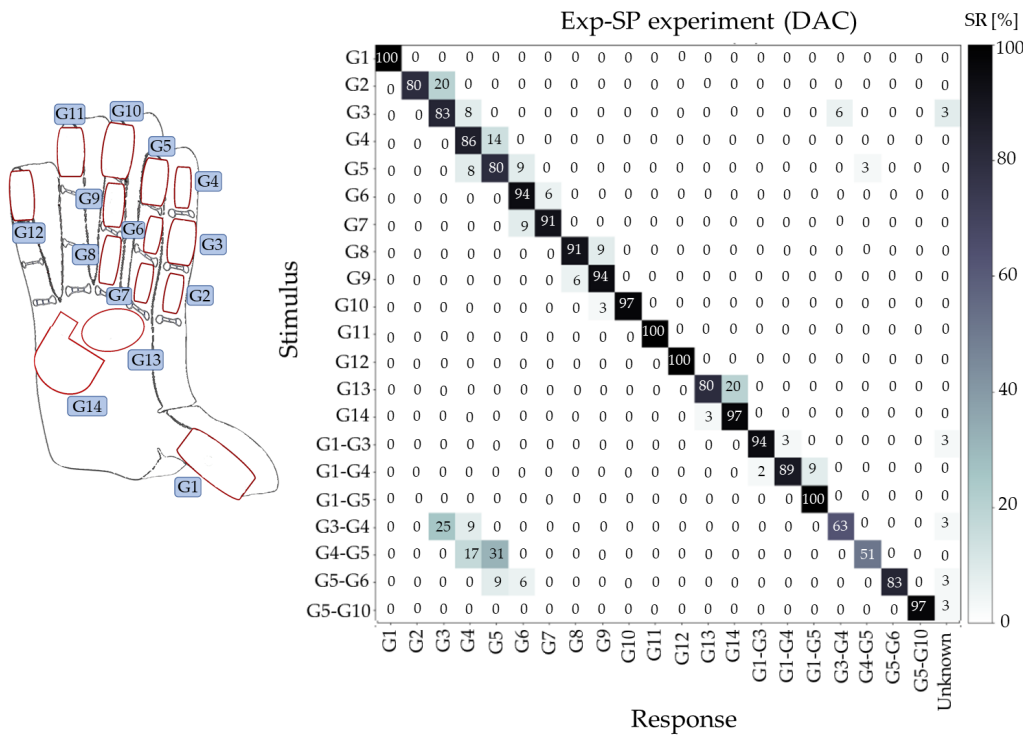


Figure 9. Left: sensing groups on the hand. Right: Confusion matrix for Exp-SP experiment.

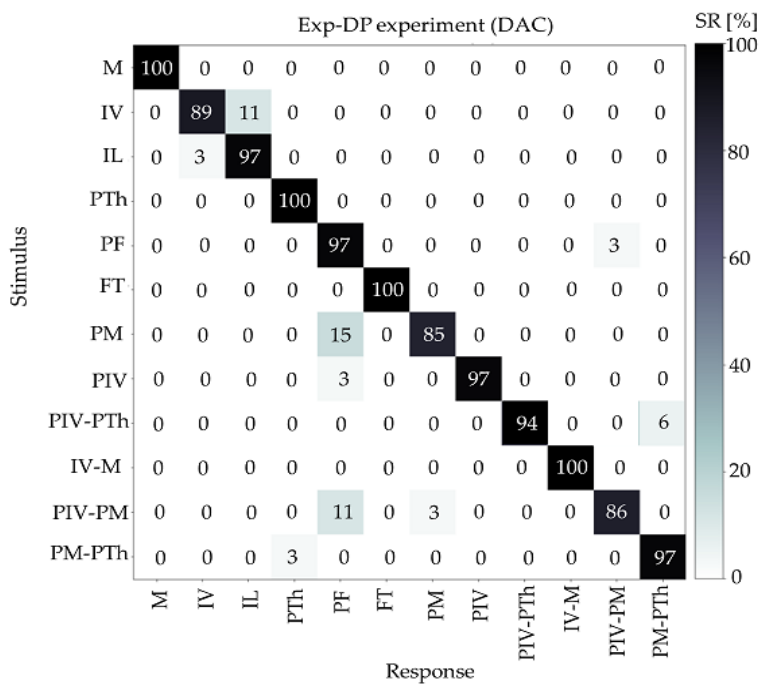


Figure 10. Confusion matrix for Exp-DP experiment.

With DAC, the subjects were more successful ($p < 0.05$) when recognizing single touches (90{7.14} %) compared to recognizing double touches (85{20} %). Importantly, the subjects could easily differentiate if the touch was single versus double (SR of 95.23{3.81} %). The dynamic patterns (Exp-DP experiment) were recognized with a high success rate (93.3{5} %).

The confusion matrix for Exp-SP test with DAC is shown in figure 9. The ‘unknown’ class was introduced to indicate that in few trials the subjects reported a group combination (multiple touches) that did not exist in the experiment (e.g., G2-G3). The confusion matrix exhibits a dominant diagonal line demonstrating that subjects could reliably recognize the applied single and double touches in most cases, where the latter were slightly more difficult to estimate correctly. When the subjects were wrong for the single touch (G1, .., G14), they mostly pointed to a directly neighbouring group placed distally or proximally with respect to the correct group (G3 to G4, G5 to G6 etc.), see the second parallel diagonals above and below the main diagonal. Excluding the misrecognition registered for G3 (predicted as G2-G3, 1 out of 35 trials, i.e. 3%), most of the “unknown” predictions were registered for double touches where the subjects predicted one group correctly while misrecognizing the second group. The confusion matrix exhibited higher diagonal values for double touches that involve groups from different fingers (e.g., G1-G5, G5-G10) compared to groups residing on the same finger (e.g., G3-G4, G4-G5). Importantly, the mistakes were typically confined to groups within the same finger (see bottom left of figure 9). Interestingly, in a few cases, double touches were mistakenly interpreted by the subjects as a single touch. For example, applying touch at G3 and G4 simultaneously (G1-G4) was mostly mistaken for G3 only.

The confusion matrix for Exp-DP test with DAC is shown in figure 10. In some trials, the subjects confused “IL” line with “IV” line and “PM-PIV” line with “PF”, and this was likely because the experimenter would occasionally activate sensors that did not belong to the target line due to the natural variability when executing the sliding patterns. The subjects made most errors when discriminating two simultaneous sliding patterns (IV-M, PIV-PM, PIV-PTh, PM-PTh).

6. Discussion and Conclusion

In this study, we presented and evaluated a high-density tactile feedback system for human-machine interfacing. The system comprises 57 distributed tactile sensors (e-skin) integrated on the fingers and palm of the robotic hand mockup, multichannel embedded electronics and a distributed electrotactile stimulation interface placed on the volar side of the subject hand. It is worth noting that sensors have been distributed on such areas that are expected to be more relevant functionally, e.g. the fingertips or areas activated when closing the hand using different grasp types (e.g., pinch, lateral grasp, palmar grasp). The contact information captured by the electronic skin was delivered to the subject through a matrix electrode comprising 64 stimulation pads distributed over the fingers and the palm of the subject's hand. The experiments have been conducted to validate the operation of the sensing component (electronic skin and embedded electronics) as well as to test the ability of the full feedback interface to acquire and transmit the mechanical interaction (applied on the electronic skin) to the subjects' hand.

The validation of the sensing component demonstrated that the e-skin and the embedded electronics can indeed detect mechanical indentation on the e-skin surface, centred on different sensors and applied sequentially and simultaneously (*static* patterns), as well as contacts sliding across the e-skin (*dynamic* patterns). Such mechanical stimuli are the basic building blocks for more complex tactile interactions that arise during functional activities.

The design and placement of the anode is an important issue for the practical application, especially when the feedback is delivered to a confined area (subject hand), and both approaches (*distributed* vs *single* anode) tested in the present study were used before in the literature [25,66]. In general, the anode should be substantially larger in size compared to a cathode, as it should serve only as a return path for the current without eliciting sensations. The "distributed" anode is a compact solution, as the anode is "within" the stimulating electrode, but the drawback is that each anode requires a single pad, strongly reducing the number of available pads to elicit sensations. Nevertheless, the conducted experiments demonstrated that this approach (DAC) resulted in significantly higher performance compared to a single anode placed on the hand dorsum (SAC). More specifically, the SAC negatively impacted on the ability of the subjects to predict static and especially double contacts. They had difficulties to distinguish between neighboring groups, particularly when stimulating the index finger. A strong spreading of sensations was reported by most subjects. Contrarily, when using DAC, the subjects predicted single and double contacts with high success rates, and they reported a well localized sensation. DAC has been therefore selected to complete the experimental campaign.

The psychometric experiments with DAC demonstrated that the online feedback conveyed by the developed system allowed the subjects to identify contact patterns delivered to the most important functional areas of the hand, including the lateral and volar side of the index finger, fingertips of all fingers and thumb, and the palm. This included simple patterns, such as contact on a single area, as well as more complex sensations arising from simultaneous touches on two areas, single and double sliding contacts, and comprehensive patterns activating many pads simultaneously. Importantly, the subjects could identify these interaction patterns despite they included natural variability due to slight variations in the way the experimenter touched the skin (e.g., inconsistent timing, different pad activations). While we have previously demonstrated that such patterns can be perceived from a single finger [63], in the present work we show that the electrotactile stimulus can be delivered to a larger area, following mechanical interactions across the whole hand. An important point is that the current system provided somatotopic feedback, which is expected to facilitate perception and interpretation of the stimulus [80]. In combination with the validation of the sensing system, the psychometric assessment demonstrates that the developed system not only detects a variety of tactile interactions but can also create tactile sensations that allow the subjects to correctly perceive and interpret such interactions, after only a brief familiarization with the system. This is an encouraging outcome implying that the novel system might be able to provide a functionally relevant feedback that can assist the subject while using a robotic hand, e.g., in slip detection and prevention [81] or for estimation of

objects properties such as compliance, hardness, texture by using exploratory motions [82–84]. Importantly, the proposed technology is versatile as it is not constrained to a specific robotic hand. While the sensing system was developed to sensorize the Michelangelo hand, the modular approach that we propose can be adapted to fit other prosthetic or robotic hands. The setup presented in this manuscript is convenient for application in a tele-manipulation scenario, while Michelangelo robotic prosthesis was used only as an example of a robotic hand. Importantly, the present work demonstrates the technology that is versatile, and can be easily adapted across different applications. To this aim, the sensing patches and the stimulation electrodes can be printed to fit other prosthetic or robotic hands (e.g., ShadowHand [85]). Finally, when considering prosthetic applications, the use of electrotactile stimulation is not a constraint as there are compact solutions that can deliver the stimulation while simultaneously recording the electrical muscle activity [86]. Likewise, the electrodes can be easily printed in different geometries so that they can be applied to different parts of the body (e.g., a rectangular and/or circular matrix electrode to be placed on the residual limb of an amputee subject).

To summarize and conclude, in the present study we proposed a system that provides spatially distributed feedback to the whole hand using a dense matrix of sensing and stimulation pads and we demonstrated its applicability by conducting experiments in able-bodied subjects. To the best of our knowledge, this is the first feedback system that can convey high-density tactile information to the whole hand using electrotactile stimulation. The provided feedback could improve utility and performance, as well as facilitate the feeling of embodiment and immersion in human-machine interfacing across fields, from teleoperation and prosthetics to virtual reality and gaming. The touch patterns tested in the presented study were limited to passive touches because the sensing system was integrated on the static mockup. Nevertheless, even a passive touch has its own relevance, especially considering psychological impact of feedback [87]. However, the future work will focus on the mounting of the sensing system onto a robotic hand, which will open up the possibility to assess the system during functional tasks (e.g., active touch). In this case, the provided feedback might allow the subject to perceive high-fidelity information such as object shape, compliance, and texture. An important future step is also to improve data processing so that more information can be extracted from the recorded tactile signals (e.g., contact pressure). All in all, this is an important step towards implementing a full high-bandwidth human machine interface that will allow a bidirectional connection between the subject and a machine (robotic system) for dexterous control and comprehensive feedback [31]. To this aim, the system described here could be supplemented with an interface that provides high density recording of electrical muscle activity. The latter can be used to decode the subject motion intention and translate those into commands for the robot [88]. Importantly, the recording of EMG could be realized through the same electrode technology as the one used in the present study to implement stimulation [86].

Ethics. The studies involving human participants were reviewed and approved by Region Liguria Ethical Committee (approval ID 172REG2016, approval date September 13, 2016 – amendment 1 approved on March 30, 2021). The participants provided their written informed consent to participate in this study.

Data Accessibility. Data supporting the results of this study are available from the authors upon reasonable request.

Authors' Contributions. YA developed and validated the system, carried out the experiments, performed the data analysis, conceived and designed the study, and drafted the manuscript. SD and MV contributed to the study design and data interpretation. LS designed the sensing arrays and contributed to the study design. All authors conceived the system, revised the manuscript and approved the submitted version.

Competing Interests. The author(s) declare that they have no competing interests

Funding. The authors acknowledge financial support from TACTile feedback enriched virtual interaction through virtual reality and beyond (Tactility) project: EU H2020, Topic ICT-25-2018-2020, RIA, ProposalID 856718 and the project ROBIN (8022-00243A) funded by the Independent Research Fund Denmark.

Acknowledgements. The authors would like to thank Erik Hernandez for providing the Tactility stimulator and for his help in implementing its communication protocol. Matija Strbac is acknowledged for his contribution to the design of the multi pad electrodes. Finally, the authors thank Moustafa Saleh for arranging the embedded electronics.

References

1. van der Meijden OAJ, Schijven MP.
The value of haptic feedback in conventional and robot-assisted minimal invasive surgery and virtual reality training: a current review.
Surgical Endoscopy. 2009 jun;23(6):1180-90.
Available from: <http://link.springer.com/10.1007/s00464-008-0298-x>.
2. Bach-y Rita P, W Kercel S.
Sensory substitution and the human-machine interface.
Trends in Cognitive Sciences. 2003 dec;7(12):541-6.
Available from: <https://linkinghub.elsevier.com/retrieve/pii/S1364661303002900>.
3. Kourtesis P, Argelaguet F, Vizcay S, Marchal M, Pacchierotti C.
Electrotactile feedback for hand interactions: A systematic review, meta-analysis, and future directions. 2021 may;1-15.
Available from: <http://arxiv.org/abs/2105.05343>.
4. MA Z, Ben-Tzvi P.
RML Glove—An Exoskeleton Glove Mechanism With Haptics Feedback.
IEEE/ASME Transactions on Mechatronics. 2015 apr;20(2):641-52.
Available from: <http://ieeexplore.ieee.org/document/6750032/>.
5. Mavroidis C, Pfeiffer C, Celestino J, Bar-Cohen Y.
Design and Modeling of an Electro-Rheological Fluid Based Haptic Interface.
In: Volume 7A: 26th Biennial Mechanisms and Robotics Conference. American Society of Mechanical Engineers; 2000. p. 653-60.
Available from: <https://asmedigitalcollection.asme.org/IDETC-CIE/proceedings/IDETC-CIE2000/35173/653/1093762>.
6. Blake J, Gurocak HB.
Haptic Glove With MR Brakes for Virtual Reality.
IEEE/ASME Transactions on Mechatronics. 2009 oct;14(5):606-15.
Available from: <http://ieeexplore.ieee.org/document/4806267/>.
7. Erwin A, O'Malley MK, Ress D, Sergi F.
Kinesthetic Feedback During 2DOF Wrist Movements via a Novel MR-Compatible Robot.
IEEE Transactions on Neural Systems and Rehabilitation Engineering. 2017 sep;25(9):1489-99.
Available from: <https://ieeexplore.ieee.org/document/7763863>.
8. Son B, Park J.
Haptic Feedback to the Palm and Fingers for Improved Tactile Perception of Large Objects.
In: Proceedings of the 31st Annual ACM Symposium on User Interface Software and Technology. New York, NY, USA: ACM; 2018. p. 757-63.
Available from: <https://dl.acm.org/doi/10.1145/3242587.3242656>.
9. Jo I, Park Y, Kim H, Bae J.
Evaluation of a Wearable Hand Kinesthetic Feedback System for Virtual Reality: Psychophysical and User Experience Evaluation.
IEEE Transactions on Human-Machine Systems. 2019 oct;49(5):430-9.
Available from: <https://ieeexplore.ieee.org/document/8736834>.
10. Margineanu D, Lovasz EC, Gruescu CM, Ciupe V, Tatar S.
5 DoF Haptic Exoskeleton for Space Telerobotics – Shoulder Module.
In: Mechanisms and Machine Science. vol. 52. Springer Netherlands; 2018. p. 111-20.
Available from: http://link.springer.com/10.1007/978-3-319-60702-3_12.

11. Schoonmaker RE, Cao CGL.
Vibrotactile force feedback system for minimally invasive surgical procedures.
In: 2006 IEEE International Conference on Systems, Man and Cybernetics. vol. 3. IEEE; 2006. p. 2464-9.
Available from: <http://ieeexplore.ieee.org/document/4274239/>.
12. Bloomfield A, Badler NI.
Virtual Training via Vibrotactile Arrays.
Presence: Teleoperators and Virtual Environments. 2008 apr;17(2):103-20.
Available from: <https://direct.mit.edu/pvar/article/17/2/103-120/58977>.
13. Pacchierotti C, Sinclair S, Solazzi M, Frisoli A, Hayward V, Prattichizzo D.
Wearable Haptic Systems for the Fingertip and the Hand: Taxonomy, Review, and Perspectives.
IEEE Transactions on Haptics. 2017 oct;10(4):580-600.
Available from: <https://ieeexplore.ieee.org/document/7922602/>.
14. King CH, Culjat MO, Franco ML, Lewis CE, Dutson EP, Grundfest WS, et al.
Tactile Feedback Induces Reduced Grasping Force in Robot-Assisted Surgery.
IEEE Transactions on Haptics. 2009 apr;2(2):103-10.
Available from: <http://ieeexplore.ieee.org/document/4798161/>.
15. Sarakoglou I, Garcia-Hernandez N, Tsagarakis NG, Caldwell DG.
A High Performance Tactile Feedback Display and Its Integration in Teleoperation.
IEEE Transactions on Haptics. 2012;5(3):252-63.
Available from: <http://ieeexplore.ieee.org/document/6200271/>.
16. Bimbo J, Pacchierotti C, Aggravi M, Tsagarakis N, Prattichizzo D.
Teleoperation in cluttered environments using wearable haptic feedback.
In: 2017 IEEE/RSJ International Conference on Intelligent Robots and Systems (IROS). vol. 2017-Septe. IEEE; 2017. p. 3401-8.
Available from: <http://ieeexplore.ieee.org/document/8206180/>.
17. Pamungkas D, Ward K.
Immersive teleoperation of a robot arm using electro-tactile feedback.
In: 2015 6th International Conference on Automation, Robotics and Applications (ICARA). IEEE; 2015. p. 300-5.
Available from: <http://ieeexplore.ieee.org/document/7081164/>.
18. Pamungkas DS, Turnip A.
Electro-tactile Cues for a Haptic Multimedia Finger Motoric Learning System.
In: 2019 International Conference on Sustainable Engineering and Creative Computing (ICSECC). IEEE; 2019. p. 127-32.
Available from: <https://ieeexplore.ieee.org/document/8906989/>.
19. Sagardia M, Hertkorn K, Hulin T, Schatzle S, Wolff R, Hummel J, et al.
VR-OOS: The DLR's virtual reality simulator for telerobotic on-orbit servicing with haptic feedback.
In: 2015 IEEE Aerospace Conference. vol. 2015-June. IEEE; 2015. p. 1-17.
Available from: <http://ieeexplore.ieee.org/document/7119040/>.
20. Hummel J, Dodiya J, Center GA, Eckardt L, Wolff R, Gerndt A, et al.
A lightweight electrotactile feedback device for grasp improvement in immersive virtual environments.
In: 2016 IEEE Virtual Reality (VR). vol. 2016-July. IEEE; 2016. p. 39-48.
Available from: <https://ieeexplore.ieee.org/document/7504686/>.
21. Pamungkas DS, Ward K.
Tele-operation of a robot arm with electro tactile feedback.
In: 2013 IEEE/ASME International Conference on Advanced Intelligent Mechatronics. IEEE; 2013. p. 704-9.
Available from: <http://ieeexplore.ieee.org/document/6584175/>.
22. Ying M, Bonifas AP, Lu N, Su Y, Li R, Cheng H, et al.

- Silicon nanomembranes for fingertip electronics.
Nanotechnology. 2012 aug;23(34):344004.
Available from: <https://iopscience.iop.org/article/10.1088/0957-4484/23/34/344004>.
23. Kajimoto H, Inami M, Kawakami N, Tachi S.
SmartTouch - augmentation of skin sensation with electrocutaneous display.
In: 11th Symposium on Haptic Interfaces for Virtual Environment and Teleoperator Systems, 2003. HAPTICS 2003. Proceedings. IEEE Comput. Soc; 2003. p. 40-6.
Available from: <http://ieeexplore.ieee.org/document/1191225/>.
24. Pamungkas DS, Ward K.
Electro-tactile feedback system for achieving embodiment in a tele-operated robot.
In: 2014 13th International Conference on Control Automation Robotics Vision (ICARCV). vol. 2014. IEEE; 2014. p. 1706-11.
Available from: <http://ieeexplore.ieee.org/document/7064573/>.
25. Kajimoto H, Kawakami N, Tachi S, Inami M.
SmartTouch: electric skin to touch the untouchable.
IEEE Computer Graphics and Applications. 2004 jan;24(1):36-43.
Available from: <http://ieeexplore.ieee.org/document/1255807/>.
26. Kato K, Ishizuka H, Kajimoto H, Miyashita H.
Double-sided Printed Tactile Display with Electro Stimuli and Electrostatic Forces and its Assessment.
In: Proceedings of the 2018 CHI Conference on Human Factors in Computing Systems. vol. 2018-April. New York, NY, USA: ACM; 2018. p. 1-12.
Available from: <https://dl.acm.org/doi/10.1145/3173574.3174024>.
27. Withana A, Groeger D, Steimle J.
Tacttoo: A Thin and Feel-Through Tattoo for On-Skin Tactile Output Anusha.
In: Proceedings of the 31st Annual ACM Symposium on User Interface Software and Technology. New York, NY, USA: ACM; 2018. p. 365-78.
Available from: <https://dl.acm.org/doi/10.1145/3242587.3242645>.
28. Svensson P, Wijk U, Björkman A, Antfolk C.
A review of invasive and non-invasive sensory feedback in upper limb prostheses.
Expert Review of Medical Devices. 2017 jun;14(6):439-47.
Available from: <http://dx.doi.org/10.1080/17434440.2017.1332989> <https://www.tandfonline.com/doi/full/10.1080/17434440.2017.1332989>.
29. Schofield JS, Evans KR, Carey JP, Hebert JS.
Applications of sensory feedback in motorized upper extremity prosthesis: a review.
Expert Review of Medical Devices. 2014 sep;11(5):499-511.
Available from: <http://www.tandfonline.com/doi/full/10.1586/17434440.2014.929496>.
30. Bensmaia SJ, Tyler DJ, Micera S.
Restoration of sensory information via bionic hands.
Nature Biomedical Engineering. 2020 nov.
Available from: <http://dx.doi.org/10.1038/s41551-020-00630-8> <http://www.nature.com/articles/s41551-020-00630-8>.
31. Farina D, Vujaklija I, Bränemark R, Bull AMJ, Dietl H, Graimann B, et al.
Toward higher-performance bionic limbs for wider clinical use.
Nature Biomedical Engineering. 2021 may:1-13.
Available from: <https://www.nature.com/articles/s41551-021-00732-x> <http://www.nature.com/articles/s41551-021-00732-x>.
32. Stephens-Fripp B, Alici G, Mutlu R.
A Review of Non-Invasive Sensory Feedback Methods for Transradial Prosthetic Hands.
IEEE Access. 2018;6:6878-99.
Available from: <http://ieeexplore.ieee.org/document/8253455/>.

33. Sensinger JW, Dosen S.
A Review of Sensory Feedback in Upper-Limb Prostheses From the Perspective of Human Motor Control.
Frontiers in Neuroscience. 2020 jun;14(June):1-24.
Available from: <https://www.frontiersin.org/article/10.3389/fnins.2020.00345/full>.
34. Antfolk C, D'Alonzo M, Rosén B, Lundborg G, Sebelius F, Cipriani C.
Sensory feedback in upper limb prosthetics.
Expert Review of Medical Devices. 2013 jan;10(1):45-54.
Available from: <https://www.tandfonline.com/action/journalInformation?journalCode=ierd20http://www.tandfonline.com/doi/full/10.1586/erd.12.68>.
35. Marasco PD, Kim K, Colgate JE, Peshkin MA, Kuiken TA.
Robotic touch shifts perception of embodiment to a prosthesis in targeted reinnervation amputees.
Brain. 2011 mar;134(3):747-58.
Available from: <https://academic.oup.com/brain/article-lookup/doi/10.1093/brain/awq361>.
36. Jung YH, Kim J, Rogers JA.
Skin-Integrated Vibrohaptic Interfaces for Virtual and Augmented Reality.
Advanced Functional Materials. 2020 dec;2008805:2008805.
Available from: <https://onlinelibrary.wiley.com/doi/10.1002/adfm.202008805>.
37. Sundaram S, Kellnhofer P, Li Y, Zhu JY, Torralba A, Matusik W.
Learning the signatures of the human grasp using a scalable tactile glove.
Nature. 2019;569(7758):698-702.
38. Chortos A, Liu J, Bao Z.
Pursuing prosthetic electronic skin.
Nature Materials. 2016 sep;15(9):937-50.
Available from: <http://www.nature.com/articles/nmat4671>.
39. Chortos A, Bao Z.
Skin-inspired electronic devices.
Materials Today. 2014 sep;17(7):321-31.
Available from: <http://dx.doi.org/10.1016/j.mattod.2014.05.006https://linkinghub.elsevier.com/retrieve/pii/S1369702114002065>.
40. Wang C, Hwang D, Yu Z, Takei K, Park J, Chen T, et al.
User-interactive electronic skin for instantaneous pressure visualization.
Nature Materials. 2013 oct;12(10):899-904.
Available from: <http://www.nature.com/articles/nmat3711>.
41. Takei K, Takahashi T, Ho JC, Ko H, Gillies AG, Leu PW, et al.
Nanowire active-matrix circuitry for low-voltage macroscale artificial skin.
Nature Materials. 2010 oct;9(10):821-6.
Available from: <http://www.nature.com/articles/nmat2835>.
42. Kim S, Laschi C, Trimmer B.
Soft robotics: A bioinspired evolution in robotics.
Trends in Biotechnology. 2013;31(5):287-94.
Available from: <http://dx.doi.org/10.1016/j.tibtech.2013.03.002>.
43. Bao Z.
Skin-inspired organic electronic materials and devices.
MRS Bulletin. 2016 nov;41(11):897-904.
Available from: <http://link.springer.com/10.1557/mrs.2016.247>.
44. Sekitani T, Someya T.
Stretchable, Large-area Organic Electronics.

- Advanced Materials. 2010 may;22(20):2228-46.
 Available from: <http://doi.wiley.com/10.1002/adma.200904054>.
45. Wettels N, Santos VJ, Johansson RS, Loeb GE.
 Biomimetic Tactile Sensor Array.
Advanced Robotics. 2008 jan;22(8):829-49.
 Available from: <https://www.tandfonline.com/doi/abs/10.1163/156855308X314533>
46. Dahiya RS, Metta G, Valle M, Sandini G.
 Tactile Sensing—From Humans to Humanoids.
IEEE Transactions on Robotics. 2010 feb;26(1):1-20.
 Available from: <http://ieeexplore.ieee.org/document/5339133/>.
47. Rus D, Tolley MT.
 Design, fabrication and control of soft robots.
Nature. 2015 may;521(7553):467-75.
 Available from: <http://www.nature.com/articles/nature14543>.
48. Kappassov Z, Corrales JA, Perdereau V.
 Tactile sensing in dexterous robot hands — Review.
Robotics and Autonomous Systems. 2015 dec;74:195-220.
 Available from: <https://linkinghub.elsevier.com/retrieve/pii/S0921889015001621>.
49. Kim S, Shin H, Song K, Cha Y.
 Flexible piezoelectric sensor array for touch sensing of robot hand.
 2019 16th International Conference on Ubiquitous Robots, UR 2019. 2019:21-5.
50. Antfolk C, Kopta V, Farserotu J, Decotignie JD, Enz C.
 The WiseSkin artificial skin for tactile prosthetics: A power budget investigation.
 International Symposium on Medical Information and Communication Technology, ISMICT. 2014:1-4.
51. Osborn L, Kaliki RR, Soares AB, Thakor NV.
 Neuromimetic Event-Based Detection for Closed-Loop Tactile Feedback Control of Upper Limb Prostheses.
IEEE Transactions on Haptics. 2016;9(2):196-206.
52. Cranny A, Cotton DPJ, Chappell PH, Beeby SP, White NM.
 Thick-film force and slip sensors for a prosthetic hand.
Sensors and Actuators, A: Physical. 2005;123-124:162-71.
53. Cotton DPJ, Chappell PH, Cranny A, White NM, Beeby SP.
 A novel thick-film piezoelectric slip sensor for a prosthetic hand.
IEEE Sensors Journal. 2007;7(5):752-61.
54. Wang Y, Xi K, Liang G, Mei M, Chen Z.
 A flexible capacitive tactile sensor array for prosthetic hand real-time contact force measurement.
 2014 IEEE International Conference on Information and Automation, ICIA 2014. 2014;8(July):937-42.
55. Agcayazi T, McKnight M, Sotory P, Huang H, Ghosh T, Bozkurt A.
 A scalable shear and normal force sensor for prosthetic sensing.
 In: 2017 IEEE SENSORS. vol. 2017-Decem. IEEE; 2017. p. 1-3.
 Available from: <http://ieeexplore.ieee.org/document/8233977/>.
56. Kim J, Lee M, Shim HJ, Ghaffari R, Cho HR, Son D, et al.
 Stretchable silicon nanoribbon electronics for skin prosthesis.
Nature Communications. 2014 dec;5(1):5747.
 Available from: <http://www.nature.com/articles/ncomms6747>.
57. Gerratt AP, Michaud HO, Lacour SP.
 Elastomeric Electronic Skin for Prosthetic Tactile Sensation.
Advanced Functional Materials. 2015 apr;25(15):2287-95.

- Available from: <https://onlinelibrary.wiley.com/doi/10.1002/adfm.201404365>.
58. Kim DH, Lu N, Ma R, Kim YS, Kim RH, Wang S, et al. Epidermal Electronics. *Science*. 2011 aug;333(6044):838-43. Available from: <https://www.sciencemag.org/lookup/doi/10.1126/science.1206157>.
59. Pang C, Koo JH, Nguyen A, Caves JM, Kim MG, Chortos A, et al. Highly Skin-Conformal Microhairy Sensor for Pulse Signal Amplification. *Advanced Materials*. 2015 jan;27(4):634-40. Available from: <https://onlinelibrary.wiley.com/doi/10.1002/adma.201403807>.
60. Štrbac M, Belić M, Isaković M, Kojić V, Bijelić G, Popović I, et al. Integrated and flexible multichannel interface for electrotactile stimulation. *Journal of Neural Engineering*. 2016 aug;13(4):046014. Available from: <http://stacks.iop.org/1741-2552/13/i=4/a=046014?key=crossref.597e7febf8dda814bf1624d1d6b8bab2https://iopscience.iop.org/article/10.1088/1741-2560/13/4/046014>.
61. "TACTILITY – An EU H2020 Research and Innovation Action" [Online]. Available: <https://tactility-h2020.eu/> [Accessed: 2021-08-25];
62. Abbass Y, Saleh M, Ibrahim A, Valle M. Embedded Feedback System for Upper Limb Prosthetics. In: 2020 27th IEEE International Conference on Electronics, Circuits and Systems (ICECS). IEEE; 2020. p. 1-4. Available from: <https://ieeexplore.ieee.org/document/9294781/>.
63. Abbass Y, Saleh M, Dosen S, Valle M. Embedded Electrotactile Feedback System for Hand Prostheses Using Matrix Electrode and Electronic Skin. *IEEE Transactions on Biomedical Circuits and Systems*. 2021 oct;15(5):912-25. Available from: <https://ieeexplore.ieee.org/document/9522029/>.
64. Kitamura N, Chim J, Miki N. Electrotactile display using microfabricated micro-needle array. *Journal of Micromechanics and Microengineering*. 2015 feb;25(2):025016. Available from: <https://iopscience.iop.org/article/10.1088/0960-1317/25/2/025016>.
65. Ishizuka H, Suzuki K, Terao K, Takao H, Shimokawa F. Development of high resolution electrostatic tactile display. In: 2017 International Conference on Electronics Packaging (ICEP). IEEE; 2017. p. 484-6. Available from: <http://ieeexplore.ieee.org/document/7939427/>.
66. Yem V, Kajimoto H. Comparative Evaluation of Tactile Sensation by Electrical and Mechanical Stimulation. *IEEE Transactions on Haptics*. 2017 jan;10(1):130-4. Available from: <http://ieeexplore.ieee.org/document/7560603/>.
67. Fares H, Abbass Y, Valle M, Seminara L. Validation of Screen - printed Electronic Skin Based on Piezoelectric Polymer Sensors. *Sensors (Basel, Switzerland)*. 2020;20(4):26.
68. Michelangelo prosthetic hand | Ottobock US [Online]. Available: <https://www.ottobockus.com/prosthetics/upper-limb-prosthetics/solution-overview/michelangelo-prosthetic-hand/> [Accessed: 2021-03-24];
69. Arapi V, Della Santina C, Averta G, Bicchi A, Bianchi M. Understanding Human Manipulation With the Environment: A Novel Taxonomy for Video Labelling. *IEEE Robotics and Automation Letters*. 2021 oct;6(4):6537-44. Available from: <https://ieeexplore.ieee.org/document/9472990/>.

70. "Smartex srl" [Online]. Available: <http://www.smartex.it/en/our-products> [Accessed: 2021-03-27];.
71. Saleh M, Abbass Y, Ibrahim A, Valle M.
Experimental Assessment of the Interface Electronic System for PVDF-Based Piezoelectric Tactile Sensors.
Sensors (Switzerland). 2019;19(20):1-12.
72. 32-Channel, Current-Input Analog-to-Digital Converter [Online]. Available: <https://www.ti.com/lit/ds/symlink/ddc232.pdf> [Accessed: 2021-08-28];.
73. Schmitz J, Sherman JM, Hansen S, Murray SJ, Balkir S, Hoffman MW.
A Low-Power, Single-Chip Electronic Skin Interface for Prosthetic Applications.
IEEE Transactions on Biomedical Circuits and Systems. 2019;13(6):1-1.
74. "Home | Tecnalia" [Online]. Available: <https://www.tecnalia.com/en/> [Accessed: 2021-03-26];.
75. Yem V, Kajimoto H.
Wearable tactile device using mechanical and electrical stimulation for fingertip interaction with virtual world.
In: 2017 IEEE Virtual Reality (VR). IEEE; 2017. p. 99-104.
Available from: <http://ieeexplore.ieee.org/document/7892236/>.
76. Kaczmarek KA, Tyler ME, Bach-Y-Rita P.
Electrotactile haptic display on the fingertips: preliminary results.
In: Proceedings of 16th Annual International Conference of the IEEE Engineering in Medicine and Biology Society. IEEE; p. 940-1.
Available from: <http://ieeexplore.ieee.org/document/415223/>.
77. Seminara L, Capurro M, Cirillo P, Cannata G, Valle M.
Electromechanical characterization of piezoelectric PVDF polymer films for tactile sensors in robotics applications.
Sensors and Actuators, A: Physical. 2011;169(1):49-58.
Available from: <http://dx.doi.org/10.1016/j.sna.2011.05.004>.
78. Seminara L, Capurro M, Valle M.
Tactile data processing method for the reconstruction of contact force distributions.
Mechatronics. 2015;27:28-37.
Available from: <http://dx.doi.org/10.1016/j.mechatronics.2015.02.001>.
79. G Gescheider.
Psychophysics: The fundamentals, 3rd ed. - PsycNET.
In: Psychophysics: The fundamentals, 3rd ed. Lawrence Erlbaum Associates; 1997. .
80. Chai G, Zhang D, Zhu X.
Developing Non-Somatotopic Phantom Finger Sensation to Comparable Levels of Somatotopic Sensation through User Training With Electrotactile Stimulation.
IEEE Transactions on Neural Systems and Rehabilitation Engineering. 2017 may;25(5):469-80.
Available from: <http://ieeexplore.ieee.org/document/7491333/>.
81. Zollo L, Di Pino G, Ciancio AL, Ranieri F, Cordella F, Gentile C, et al.
Restoring tactile sensations via neural interfaces for real-time force-and-slippage closed-loop control of bionic hands.
Science Robotics. 2019 feb;4(27):eaau9924.
Available from: <https://robotics.sciencemag.org/lookup/doi/10.1126/scirobotics.aau9924>.
82. Geier A, Tucker R, Somlor S, Sawada H, Sugano S.
End-to-End Tactile Feedback Loop: From Soft Sensor Skin Over Deep GRU-Autoencoders to Tactile Stimulation.
IEEE Robotics and Automation Letters. 2020 oct;5(4):6467-74.
Available from: <https://ieeexplore.ieee.org/document/9152113/>.
83. Seminara L, Gastaldo P, Watt SJ, Valyear KF, Zuher F, Mastrogiovanni F.
Active Haptic Perception in Robots: A Review.

- Frontiers in Neurorobotics. 2019 jul;13(July):1-20.
Available from: <https://www.frontiersin.org/article/10.3389/fnbot.2019.00053/full>.
84. Yi Z, Zhang Y, Peters J.
Bioinspired tactile sensor for surface roughness discrimination.
Sensors and Actuators, A: Physical. 2017;255:46-53.
Available from: <http://dx.doi.org/10.1016/j.sna.2016.12.021>.
85. "Dexterous Hand Series – Shadow Robot Company" [Online]. Available: <https://www.shadowrobot.com/dexterous-hand-series/> [Accessed: 2021-12-22];.
86. Garenfeld MA, Jorgovanovic N, Ilic V, Strbac M, Isakovic M, Dideriksen JL, et al.
A compact system for simultaneous stimulation and recording for closed-loop myoelectric control.
Journal of NeuroEngineering and Rehabilitation. 2021 dec;18(1):87.
Available from: <https://doi.org/10.1186/s12984-021-00877-5>.
87. Beckerle P, Kõiva R, Kirchner EA, Bekrater-Bodmann R, Dosen S, Christ O, et al.
Feel-Good Robotics: Requirements on Touch for Embodiment in Assistive Robotics.
Frontiers in Neurorobotics. 2018 dec;12(December):1-7.
Available from: <https://www.frontiersin.org/article/10.3389/fnbot.2018.00084/full>.
88. Ison M, Vujaklija I, Whitsell B, Farina D, Artermiadis P.
High-Density Electromyography and Motor Skill Learning for Robust Long-Term Control of a 7-DoF Robot Arm.
IEEE Transactions on Neural Systems and Rehabilitation Engineering. 2016 apr;24(4):424-33.
Available from: <https://ieeexplore.ieee.org/document/7073629/>.